A Diffraction Ray Tracing Method Based on Curved Surface Ray Tube for Complex Environment

Dan Shi, Na Lv, and Yougang Gao

School of Electronic Engineering
Beijing University of Posts and Communications, Beijing, 100876, China
shidan@buptemc.com

Abstract ─ A self-adaptive ray tracing method for predicting radio propagation based on the curved surface ray tube (CSRT) model is proposed in this paper. The CSRT model is implemented in the ray tracing method to reduce the unnecessary consume compared with the four-ray tube model in complex environments. Both the theoretical calculation and the practical simulation were applied to verify the high efficiency of the CSRT model. The radio wave propagation in a complex scene was calculated by the CSRT model and the four-ray tube model, and the theoretical analytical result demonstrated that the CSRT model achieved a speed up of 4 times compared to the four-ray tube model. Moreover, the wave propagations in several different environments were simulated with our developed software based on the CSRT and four-ray tube tracing method, and the comparisons of the simulation time spent by the two methods proved the high efficiency of the CSRT model. In addition, the correct prediction of the propagation paths and E-field also validates the accuracy of the CSRT model.

Index Terms ─ CSRT model, four-ray tube, radio wave propagation, ray tracing.

I. INTRODUCTION

In recent years, wave propagation prediction in the electrically large environment has been studied in an extensive published literature. A considerable interest has been shown in the ray tracing algorithm researches combined with the uniform theory of diffraction (UTD) [1-6]. Compared with the high accuracy but time-consuming reverse algorithm, the time-saving shooting and bouncing ray (SBR) method [7-12] has attracted attentions widely.

A ray tracing method based on the geometrical optics (GO) theory was presented to predict reflection and refraction rays [13-15]. A center-ray tube model was used in [14], which set one ray as the center of a ray cone and predicted the propagation of electromagnetic waves by only tracing the center ray of the tube. Since the wavefront of a center-ray tube is a circle or an ellipse, it overlaps with another wavefront when it is used to cover the spherical surface. Moreover, the radius of the receiving ball also determines the accuracy, and this model may produce abundant repeated paths. The lateral-ray tube model used in [5-8,14] is a good solution to the overlapping problem. The icosahedron model [7,8] and point source launching four-ray tube model [5,6,14] can cover the spherical wavefront seamlessly and without overlapping. Since the models mentioned before cannot be applied to trace diffraction rays, a segment source launching four-ray tube model combined with the UTD was proposed in [5,6]. This model solved the difficulties of the point source launching ray tube in tracing diffraction paths, and the cylindrical wavefront can be covered seamlessly and without overlap. Nevertheless, the segment source launching four-ray tube model cannot deal with complex crossing situations with the terrain and may produce much extra expending. Thus, a triangular wavefront ray tube model has been mentioned in the paper [16], but there are not detailed descriptions about the features and its application in tracing processing.

On this basis, a three-ray curve surface ray tube (CSRT) model is presented in this paper, and the tracing process is introduced in detail using this model. The CSRT model can be applied to predict the propagation of the diffraction rays. Compared with the segment source launching four-ray tube model (hereinafter referred as four-ray tube model), the CSRT model can deal with more general situations accurately with less consumptions. Thus, the CSRT model can provide accurate prediction outcomes with high efficiency in more general environments.

Section II gives a detailed definition of the three-ray CSRT model, and proves the efficiency improvement of the CSRT model in theory compared with the four-ray tube model. In Section III, different intersection situations with the terrain triangle facets by using the CSRT are listed. The description of how the tracing method runs is described in Section IV. Section V shows several simulation results of different terrains, and discusses the results compared between the three-ray CSRT model and the four-ray tube model tracing method. In Section VI, a

Submitted On: November 24, 2016
Accepted On: January 28, 2017

conclusion is drawn.

II. COMPARISONS BETWEEN THE FOUR-RAY TUBE MODEL AND THE THREE-RAY CSRT MODEL

The four-ray tubes launched by edges are shown in Fig. 1 (a). Every two adjacent rays of the four-ray tubes determining a ray tube are in the same plane, which meets the characteristic of the conventional lateral-ray tube. The four-ray tube model is suitable to calculate the wave propagation in the simple city environments. The buildings in city models are usually assumed to be cubes (Fig. 1 (b)), and if the four-ray tube model partly crosses with a building, the wavefront of the tube ABCD will be divided into two quadrilaterals. However, only the wavefront BCFE can produce a reflection ray tube. Since the edges of two buildings are parallel, the rays IE and JF are in the same plane. So, rays IE, IB, JC and JF can form a new four-ray tube for reflection.

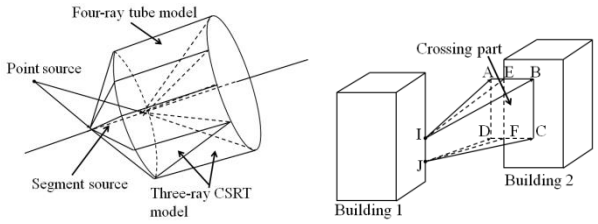

Fig. 1. (a) The four-ray tubes and three-ray CSRTs launching model. (b) The four-ray tube model in the city environment.

However, for the complex environment, the terrain is often represented as closely spaced triangular surface. The situations of the ray tube crossing with a terrain become more complex. In Fig. 2, the wavefront of the four-ray tube launched from the diffraction edge is divided into two parts. Nevertheless, the intersecting part of the wavefront cannot produce one or several four-ray tubes. Thus, the popular solution is to assume the whole tube will reflect from the plane of the terrain triangular. The part to complete the four-ray tube wavefront does not produce real rays, so rays in this part belong to the unnecessary redundancy. When the reflection ray tube crosses with the terrain again, the intersecting situations become more complex, and the consumptions increase significantly. Many paths which do not exist will be counted in the result.

In Fig. 2, the edge AB is the mirror edge of the diffraction edge of the terrain triangle, and the point O is the crossing point of line AC and line BE, which is regarded as the virtual launching point of this four-ray tube.

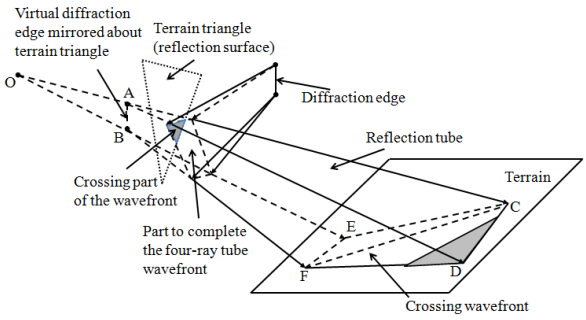

Fig. 2. The four-ray tube reflects on the terrain triangle and crosses with the terrain.

Parameters in Fig. 2 can be expressed as $OA = H_1$, $OB = H_2$, $AC = L_{11}$, $AD = L_{12}$, $BE = L_{21}$, $BF = L_{22}$, $AB = W$, $\angle AOB = \theta$, $\angle CAD = \angle \mathrm{EBF} = \alpha$. Use z to represent the length of the segment CF. According to the geometric principle, z can be calculated by the Equation (1):

$$z = \sqrt{{x_4}^2 + x_1 x_2 + \frac{x_2({x_3}^2 - {x_2}^2)}{x_2 - x_1}}, \tag{1}$$

where

$$\begin{cases} x_1 = \frac{W(L_{11}+H_1)}{H_1} \\ x_2 = \frac{W(L_{22}+H_2)}{H_2} \\ x_3 = \sqrt{\frac{{H_2}^2{L_{11}}^2}{{H_1}^2} + {L_{22}}^2 - \frac{2H_2 L_{11} L_{22}}{H_1}\cos\alpha} \\ x_4 = \sqrt{\frac{{H_1}^2{L_{22}}^2}{{H_2}^2} + {L_{11}}^2 - \frac{2H_1 L_{11} L_{22}}{H_2}\cos\alpha} \end{cases}. \tag{2}$$

The sides of the quadrilateral CDFE are supposed that $CD = y_1$, $DF = y_2$, $EF = y_3$, $CE = y_4$, and the value of them can be calculated with Equation (3):

$$\begin{cases} y_3 = \sqrt{{L_{11}}^2 + {L_{12}}^2 - 2L_{11}L_{12}\cos\alpha} \\ y_2 = \sqrt{(L_{12}+H_1)^2 + (L_{22}+H_2)^2 - 2(L_{12}+H_1)(L_{22}+H_2)\cos\theta} \\ y_3 = \sqrt{{L_{21}}^2 + {L_{22}}^2 - 2L_{21}L_{22}\cos\alpha} \\ y_4 = \sqrt{(L_{11}+H_1)^2 + (L_{21}+H_2)^2 - 2(L_{11}+H_1)(L_{21}+H_2)\cos\theta} \end{cases}. \tag{3}$$

The area of the wavefront CDEF is expressed as S_f. Hence,

$$S_f = \sqrt{p_1(p_1 - y_1)(p_1 - y_2)(p_1 - z)} + \sqrt{p_2(p_2 - y_3)(p_2 - y_4)(p_2 - z)}, \tag{4}$$

where

$$\begin{cases} p_1 = \frac{1}{2}(y_1 + y_2 + z) \\ p_2 = \frac{1}{2}(y_3 + y_4 + z) \end{cases}. \tag{5}$$

If the area of every terrain triangle is a, the crossing situation cannot be processed directly when the area of the wavefront of a ray tube is larger than a. So, the ray tube should be subdivided into several new ray tubes with smaller wavefront, and the number of the new ray tubes for every subdivision is c. Provided that every subdivision time is t_1 and the intersection time of every

ray tube is t_2, the processing time of this ray tube for the intersection T_f can be expressed as follows:

$$T_f = \left\lceil \frac{ln\left\lceil \frac{S_f}{a} \right\rceil}{ln\, c} \right\rceil t_1 + \left\lceil \frac{S_f}{a} \right\rceil t_2. \quad (6)$$

However, since the ratio of the crossing part of the wavefront on the terrain triangle to the completed wavefront is r, the ratio of the area of the shadow on the quadrilateral CDFE to the area of the wavefront CDFE is also r. So, only the rays crossing with the shadow part in the four-ray tube are real rays produced by reflection.

To reduce the unnecessary cost, we define a CSRT model in which every two adjacent rays in a ray tube are not required to be in the same plane. So the profile of a CSRT could be a curve surface. All the rays in the CSRT model must be launched by a same diffraction edge, and there will be a common virtual point source for them. In this paper, the three-ray CSRT model is introduced.

The three-ray CSRT model is produced by connecting the opposite vertex of the quadrilateral wavefront to divide the four-ray tube into two ray tubes with triangular wavefront (Fig. 1 (a)), so the wavefront of the three-ray CSRTs launched from an edge can also cover the cylindrical diffraction wavefront. The CSRT model in Fig. 3 is launched from diffraction edge AB. Supposing that the rays AC and BD are in the same plane, so the ray AE is in the different plane with ray BD. The profile ABDE is a curve surface consisted of the rays launched from the edge AB to the line DE. For all the rays in this tube, there must be a common virtual launch point before the diffraction. Combined with the UTD, diffraction rays in CSRT launched by edge AB will never cross with each other during the propagation process (except the points on the edge AB). So there will be no rays passing through the curve surface and go into another ray tube, which proves the three-ray CSRT model to be appropriate for wave propagation prediction.

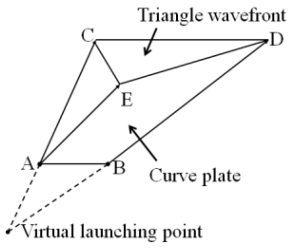

Fig. 3. The CSRT model.

The CSRT model has no strict requirements on whether the adjacent rays are in the same plane. So when a three-ray CSRT intersects with the terrain triangles, no matter what the shape of the intersection wavefront is, it always can be divided into some triangle wavefronts. Thus, all the rays in reflection three-ray tubes are real rays produced by reflection.

If the CSRT model is used in Fig. 2, only the crossing part will reflect. The crossing part of the wavefront of the CSRT and the terrain is the shadow part exactly. So the area of the wavefront of the CSRT S_{CSRT} is:

$$S_{CSRT} = rS_f, \quad (7)$$

and the handling time T_{CSRT} of the CSRT method can be calculated as follows:

$$T_{CSRT} = \left\lceil \frac{\ln\left\lceil \frac{S_{CSRT}}{a} \right\rceil}{\ln c} \right\rceil t_1 + \left\lceil \frac{S_{CSRT}}{a} \right\rceil t_2. \quad (8)$$

So, the time ratio of the four-ray tube and the three-ray CSRT is indicated as:

$$\eta = \frac{T_f}{T_{CSRT}}. \quad (9)$$

The parameters and the constants in the Equations (1) - (8) are assumed as the following values: $H_1 = H_2 =$ 10 m, $L_{11} = L_{21} = 10000\ m$, $L_{12} = L_{22} = 1000\ m$, $W = 10\ m$, $\theta = \pi/3$, $\alpha = \pi/6$, $r = 1/4$, $a = 100\ m^2$, $c = 4$. It can be calculated that $T_f = 10t_1 + 438831t_2$, $T_{CSRT} = 9t_1 + 109708t_2$. Since that t_1 is very small and can be ignored when compared with t_2, it is concluded that $\eta \approx 4$.

Thus, the calculation efficiency of the three-ray CSRT model has been increased by 4 times compared with the four-ray tube model in the above scenario. It is an efficient way with the CSRT model for ray tracing process in the complex terrain.

III. DIFFRENT SITUATIONS OF RAY TUBE CROSSING WITH THE TERRAIN

When a CSRT crosses with terrain triangles, there will be several different crossing situations for the wavefront of the ray tube. The three-ray CSRT model can self-adaptively deal with the situations as follows.

A. Completely crossing

When the three-ray CSRT model intersects with a terrain triangle completely (Fig. 4 (a)), all the rays in the tube will reflect from this triangle. It just needs to obtain the reflection rays of the three rays AC, AD and BE to form the new reflection three-ray CSRT. At the same time, it is also necessary to get mirror point O' of O about the terrain triangle as well as mirror edge A'B'. O' and A'B' will be applied to the next tracing step as virtual launching point and virtual launching edge.

B. Partly crossing with a terrain triangle

When the ray tube partly intersects with a terrain triangle, different treatments will be applied to different situations of intersection. If the wavefront of the intersecting part is triangular, it only needs to find the diffraction points of the vertexes of the triangular wavefront and to restructure the three-ray CSRT. For the new CSRT, a reflection ray tube can be produced according to the steps of Subsection A. However, if the

wavefront of the intersecting part is not a triangle, the ray tube should be segmented. The polygon wavefront can be divided into several triangular wavefronts. In Fig. 4 (b), the wavefront of the crossing part is an irregular polygon DEGH. The irregular polygon wavefront is divided into two triangular DEH and EGH by connecting points H and E. Find the diffraction points A and G of the new vertexes of wavefronts H and G on the edge AB, and two CSRTs determined by rays AH, AD, BE and rays AH, FG, BE are formed. The reflection ray tubes of this two new CSRTs can be produced based on the treatment in Subsection A.

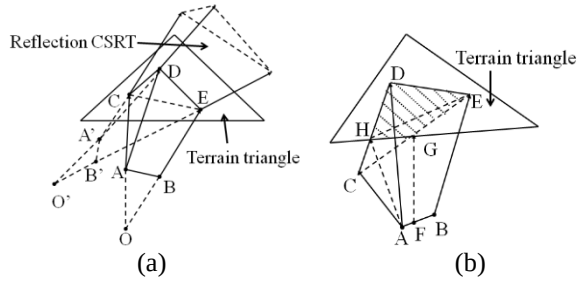

Fig. 4. (a) Completely crossing with terrain triangle. (b) Partly crossing with a terrain triangle.

C. Intersecting with adjacent terrain triangles

When the ray tube intersects with two adjacent terrain triangles (Fig. 5 (a)), the wavefronts CFG and DEGF are on two terrain triangles, so the two wavefronts can be treated as method in Subsection B respectively.

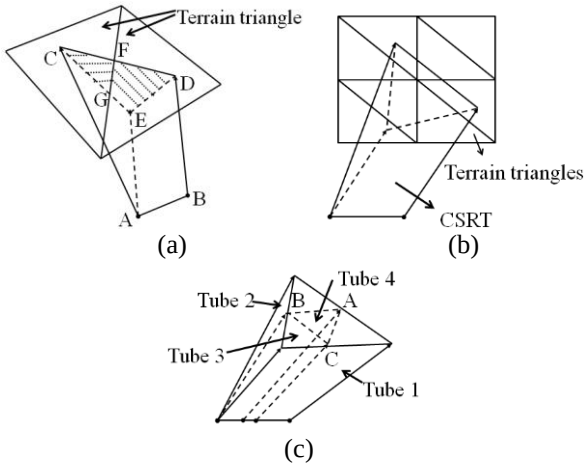

Fig. 5. (a) Crossing with two terrain triangle. (b) Crossing with several terrain triangles. (c) Subdivide ray tube.

D. Intersecting with several terrain triangles

If the ray tube intersects with several terrain triangles (Fig. 5 (b)), since the terrain triangles are not closely associated, it is difficult to determine the specific situations of intersection usually. To reduce the complexity of crossing situations, it is necessary to get the ray tube segmented. First, we suppose a wavefront of the three-ray CSRT, and then get the midpoints of each edge of it (Fig. 5 (c)). Connection of the midpoints A, B and C will divide the triangle wavefront into four triangles. Next, we get the launching points of these three points on the launching edge, so the ray tube will be segmented into four new three-ray CSRTs with smaller wavefronts.

IV. RAY TRACING PROCESS

The three-ray CSRT model proposed in this paper is mainly used to trace diffraction rays. So the actual ray tracing process considering transmission and reflection should combine this model with the point source launching three-ray tube model. For simplification, this paper only considers the situations in which only one diffraction and multiple reflections occur. The flow chart of the ray tracing is shown as Fig. 6.

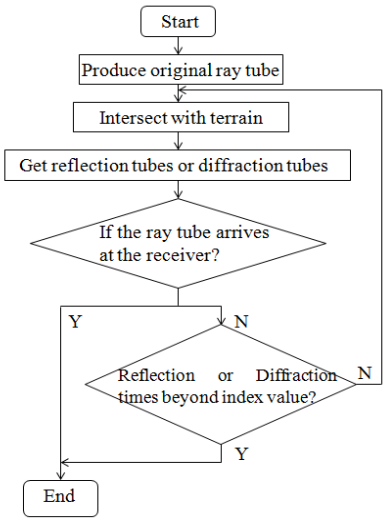

Fig. 6. The flow chart of the ray tracing.

A. Produce initial ray tube

The initial point source launching three-ray rubes are generated through the icosahedron method proposed by [8]. During the process of tracing, all the ray tubes will have triangular wavefronts and same crossing situations with the terrain triangles. So different kinds of ray tubes can be processed in a unified way.

B. Diffraction and reflection

The initial ray tubes or the high order reflection ray tubes will diffract from the crossing lines of the terrain triangles if the lines are diffraction edges, so the three-ray CSRTs will be produced. Besides, the other parts of these ray tubes crossing with terrain will reflect from the terrain and produce reflected ray tubes.

C. Judgment of the reception

During the ray tracing, it should be determined whether the ray tube illuminates the receiver. The ray tube illuminates the receiver when the receiver is in the area covered by the ray tube and the ray tube does not cross with other terrain triangles before arriving it.

V. SIMULATIONS AND COMPARISONS

The simulation software was developed by putting the ray tracing process based on the CSRT model and the four-ray tube model into the codes. Simulation results of several different terrains using this software are displayed in this part. The typical terrain formed by several terrain triangles and the actual complex terrain from the electric map were both investigated.

In Fig. 7, there are two parallel diffraction edges in the terrain. A transmitter (Tx (17.86, 576.55, 223.46)) and a receiver (Rx (330.89, 269.15, 172.70)) were placed on the terrain. The distance between the Tx and the Rx is 441.65 m. The paths simulated by the tracing methods based on the CSRT model and the four-ray tube model are exactly same, which are shown in Fig. 7. There are 7 paths totally, which are in accord with the theoretical result obviously. From Fig. 7 we can see that several diffraction paths are included, which prove that the CSRT model works well in predicting diffraction paths.

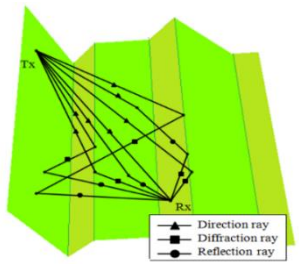

Fig. 7. Terrain with parallel diffraction edges.

The terrain in Fig. 8 is same as that in Fig. 7. The only difference is that one of the diffraction edges in Fig. 8 is rotated so that the two diffraction edges are not parallel. All the 5 possible paths are predicted and displayed in Fig. 8. The method based on the CSRT model is accurate and applicable in different diffraction environment.

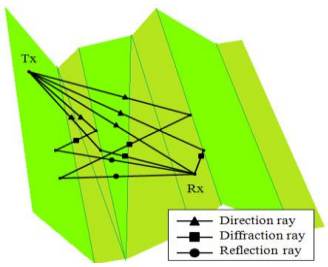

Fig. 8. Terrain with nonparallel diffraction edges.

Table 1 shows the computational time and E-field at the point of Rx in four different environments simulated by the CSRT model tracing method and the conventional four-ray tube model tracing method. The excitation frequency is 1000 MHz. In the Table 1, the Terrain 3 and the Terrain 4 are both actual environment cut from the real electric map. The size of the Terrain 3 is 2×2.2 km^2 (from 42°19'26.6035"N and 82°50'25.8125"E to 42°18'25.7818"N and 82°52'4.7458"E), and the distance between the Tx and the Rx was 609.63 m. The size of the Terrain 4 is 9.5×10 km^2 (from 42°21'31.6139"N and 82°48'28.3466"E to 42°16'44.1722"N and 82°55'40.7631"E) and the distance between the Tx and Rx is 439.60 m.

Table 1: The comparison of calculation time and E-field

Scenario	Computational Time(s)		E-field (V/m)		Error
	The CSRT Model	The Four-Ray Tube Model	The CSRT Model	The Four-Ray Tube Model	
Fig. 7 (0.75×0.56km^2)	90	91	2.23	2.2	1.36%
Fig. 8 (0.75×0.56km^2)	116	112	1.86	1.86	0
Terrain 3 (2×2.2km^2)	1003	1683	0.95	1.01	5.94%
Terrain 4 (9.5×10km^2)	8090	9523	1.54	1.62	4.94%

The complexity of the scenarios in the Table 1 increases with the increase of the terrain size. The results show that the four-ray tube model tracing method and the CSRT model tracing method use similar computational time when they are applied in the simple scenarios in Fig. 7 and Fig. 8. However, as the scenarios become more complex, the CSRT model tracing method spent less computational time. The errors of the E-field at the point of Rx between the CSRT model and the four-ray tube model are also listed in the Table 1. The average error is only 3.06%, which proves the high accuracy of the CSRT model tracing method.

VI. CONCLUSION

This paper introduced a three-ray CSRT model, which is suitable for the diffraction calculation in ray tracing. The CSRT model is accurate and has great advantages over the segment source launching four-ray rube model in efficiency.

The algorithm presented in this paper just considers one diffraction and multiple reflections. In practice, the CSRT model can be used to calculate high order diffraction paths. When the CSRT model is used to produce high order diffraction ray tubes, the rays in new tubes may cross with others, so it is necessary to do some special treatment which can be studied in the next steps.

ACKNOWLEDGMENT

This work has been supported by National Natural Science Foundation of China, No. 61201024.

REFERENCES

[1] H.-W. Son and N.-H. Myung, "A deterministic ray tube method for microcellular wave propagation prediction model," *IEEE Trans. Antennas Propagat.*, vol. 47, no. 8, pp. 1344-1350, 1999.

[2] S. Y. Tan, M. Y. Tan, and H. S. Tan, "Multipath delay measurements and modeling for interfloor wireless communications," *IEEE Trans. Veh. Technol.*, vol. 49, no. 4, pp. 1334-1341, 2000.

[3] C. Oestges, B. Clerckx, L. Raynaud, and D. Vanhoenacker-Janvier, "Deterministic channel modeling and performance simulation of micro-cellular wide-band communication systems," *IEEE Trans. Veh. Technol.*, vol. 51, no. 6, pp. 1422-1430, 2002.

[4] G. Carluccio and M. Albani, "An efficient ray tracing algorithm for multiple straight wedge diffraction," *IEEE Trans. Antennas Propagat.*, vol. 56, no. 11, pp. 3534-3542, 2008.

[5] C. Saeidi, A. Fard, and F. Hodjatkashani, "Full three-dimensional radio wave propagation pre-iction model," *IEEE Trans. Antennas Propagat*., vol. 60, no. 5, pp. 2462-2471, 2012.

[6] C. Saeidi, F. Hodjatkashani, and A. Fard, "New tube-based shooting and bouncing ray tracing method," *Proc. IEEE ATC*, Hai Phong, Vietnam, pp. 269-273, Oct. 12-14, 2009.

[7] S.-H. Chen and S.-K. Jeng, "SBR image approach for radio wave propagation in tunnels with and without traffic," *IEEE Trans. Veh. Technol.*, vol. 45, no. 3, pp. 570-578, 1996.

[8] S.-H. Chen and S.-K. Jeng, "An SBR/image approach for radio wave propagation in indoor environments with metallic furniture," *IEEE Trans. Antennas Propagat*., vol. 45, no. 1, pp. 98-106, 1997.

[9] Y. B. Tao, H. Lin, and H. J. Bao, "Adaptive aperture partition in shooting and bouncing ray method," *IEEE Trans. Antennas Propagat*., vol. 59, no. 9, pp. 3347-3357, 2011.

[10] H. Ling, R. Chou, and S. Lee, "Shooting and bouncing rays: Calculating the RCS of an arbitrarily shaped cavity," *IEEE Trans. Antennas Propagat*., vol. 37, pp. 194-205, 1989.

[11] R. Burkholder and P. Pathak, "Computing the time domain EM scattering from large open-ended cavities using the SBR and GRE ray shooting methods," *in 9th Annual Review of Progress in Applied Computational Electromagnetics*, pp. 602-617, 1993.

[12] J. M. Baden and V. K. Tripp, "Ray reversal in SBR RCS calculations," *in 31st International Review of Progress in Applied Computational Electromagnetics*, pp. 1-2, 2015.

[13] S. Y. Seidel and T. S. Rappaport, "Site-specific propagation prediction for wireless in-building personal communication system design," *IEEE Trans. Veh. Technol.*, vol. 43, pp. 879-891, Nov. 1994.

[14] C.-F. Yang, B.-C. Wu, and C.-J. Ko, "A ray-tracing method for modeling indoor wave propagation and penetration," *IEEE Trans. Antennas Propagat*., vol. 46, no. 6, pp. 907-919, 1998.

[15] G. Liang and H. L. Bertoni, "A new approach to 3-D ray tracing for propagation prediction in cities," *IEEE Trans. Antennas Propagat*., vol. 46, no. 6, pp. 853-863, 1998.

[16] P. Bernardi, R. Cicchetti, and O. Testa, "An accurate UTD model for the analysis of complex indoor radio environments in microwave WLAN systems," *IEEE Trans. Antennas Propagat*., vol. 52, no. 6, pp. 1509-1520, 2004.

Dan Shi received her Ph.D. degree in Electronic Engineering from BUPT in Beijing, China in 2008. Now she is an Associate Professor in Beijing University of Posts and Telecommunications. Her research interests include electromagnetic environment and electromagnetic computation.

Na Lv received her Bachelor degree in Communication Engineering from BUPT in Beijing, China in 2015. Now she is studying for Master degree in Beijing University of Posts and Telecommunications in Beijing, China.

Yougong Gao received his B.S. degree in Electrical Engineering from National Wuhan University, China in 1950. He is now a Professor and Ph.D. Supervisor in Beijing University of Posts and Telecommunications, China.